Polymer brush bilayers at thermal equilibrium: A theoretical approach

Mike Edwards

edwards.ph@yahoo.com

Leibniz-Institut für Polymerforchung, Hohe Straβe 6, 01069 Dresden, Germany

Dated: November 22, 2020

ABSTRACT: By means of statistical mechanics of polymers and density functional theory (DFT), polymer brush bilayers are investigated at thermal equilibrium. Density profiles show how brushes balance compression and interpenetration when they come into contact. Normal pressure indicates that substrates might repel, attract or even do not sense each other (though the brushes interpenetrate) upon varying system parameters. The results, based on that it takes deformations of both brushes into account, suggests that existing theories about polymer brush bilayers (based on blob picture) need highly likely to be reviewed.

Keywords: Polymer brush bilayers, Density functional theory (DFT), Entropic elasticity, Steric repulsion

INTRODUCTION

Polymers are a class of long macromolecules that consist of repeated units of atoms or molecules i.e. monomers[1]. Connectivity among monomers in a polymer chain is fulfilled through sharing valance electrons i.e. covalent or molecular bond. Monomers undergoing Brownian motions, constantly, change configuration of whole polymer chain so that in long time polymer chain undergoes all possible conformations. Polymer brushes are a class of polymeric structures that are present in biology, industry and medicine[2]. Polymer brushes consist of densely grafted polymer chains onto a surface where all chains stretch in perpendicular direction due to *steric* repulsion among monomers. Two opposing brush covered surfaces form a polymer brush bilayer[2]. Polymer brush bilayers are present in a wide range of biological systems such as mammalian knee joints as lubricant and capillaries of plants[2]. There have been many theoretical, experimental and numerical approaches to polymer brush bilayers and interested readers can read a recent review and references there in[4]. In the next section, density functional (DFT) is introduced as a useful tool in investigation of polymer structures. In section , DFT is applied to polymer brush bilayers and in the last section, conclusions are discussed.

METHOD

Density functional theory (DFT) is a useful theoretical method in studying many body systems. In principle, DFT is based on describing free energy of systems in terms of their particle density and minimizing free energy with respect to density and other parameters to find equilibrium properties. In systems with *inhomogeneous* particle density, free energy is has a functional of particle density. In such cases, *variational* derivative is applied. Here, I describe constructing free energy of polymer brushes in an step by step manner. As the first step, equilibrium properties of a polymer chain is introduced with help of *N-vector* model. Then, short-ranged pair interactions between monomers are introduced by using *Virial expansion* of free energy. At the ened, free energy functional for polymer brushes is constructed and introduced.

Polymer chain in external force

Conformation of a polymer chain constantly changes due to Brownian motion of its monomers. Theoretically, this situation could be assumed as N vectors of length a which are connected to each other and are freely rotating in three dimensional space. To obtain elastic properties of the chain, we need to apply a force field on it and observe its response. At the end, one has to remove the force field from the resulting quantities. The remaining leading terms represent elastic properties of chain in absence of the external force field. First of all, I introduce Hamiltonian of the system as a summation over inner products of the external force field with all vectors as follows,

$$H = -fa \sum_{i=1}^{N} \cos\theta_i \tag{1}$$

Negative sign ensures here that minimum energy takes place when all vectors are directed parallel to the external force field. So, conformations of the polymer chain are characterized by θ, the smaller angle between force field and vectors. For simplicity and symmetry considerations, I choose spherical polar coordinates and apply an external force field in the z direction. This way, the angle between the external force field and each vector is the same as polar angle θ in spherical polar coordinates. Having introduced the Hamiltonian, the next step is to calculate the partition function which is defined as $Z = \int d\Omega \exp -H/k_{\mathrm{B}}T$ where $d\Omega = d\boldsymbol{x}_1 \ldots d\boldsymbol{x}_N$ denotes a hyper volume element in configuration space of N vectors. The partition function reduces to the following integral in spherical polar coordinates,

$$Z(f,T) = \left(2\pi a^2 \int_0^{\pi} e^{\zeta\cos\theta} \sin\theta \, d\theta\right)^N \tag{2}$$

where I introduce dimensionless quantity $\zeta = af/k_{\mathrm{B}}T$. The above integral is simply solvable due to uncorrelated vectors (monomers) and it gives the following result for the partition function,

$$Z(f,T) = \left(4\pi a^2 \frac{\sinh\zeta}{\zeta}\right)^N \tag{3}$$

Having obtained the partition function, we can simply calculate canonical free energy as $F(f,T) = -k_{\mathrm{B}}T \log Z(f,T)$ giving following expression,

$$F(f,T) = -Nk_{\mathrm{B}}T \log\left(4\pi a^2 \frac{\sinh\zeta}{\zeta}\right) \tag{4}$$

This is free energy in external force and temperature ensemble. Since, I fixed external force and temperature, so the chain length fluctuates. Expectation value of the chain length can be obtained from canonical free energy as $-\partial F(f,T)/\partial f$ which gives us the following result,

$$\langle L\rangle = Na\left(\coth\zeta - \frac{1}{\zeta}\right) \tag{5}$$

Expectation value of chain length can alternatively be calculated from direct integration which gives us the above result. Note that, in statistical mechanics, $\coth\zeta - \zeta^{-1}$ is called *Langevin* function[3]. As it is observed, expectation value of the chain length subject to an external force is non-zero. Certainly, this occurs, exclusively, along the external force direction (here the z direction) and in other directions (here x and y directions) it vanishes. To obtain fluctuations of the chain length, one needs to have expectation value of the mean-squared-length i.e. $\langle L^2\rangle$. Expectation value of the mean-squared-length can be calculated through integration which gives us the following result,

$$\langle L^2\rangle = Na^2 \tag{6}$$

and fluctuation in the chain length is calculated via $\langle L^2\rangle - \langle L\rangle^2$ giving us the following result,

$$\Delta L^2 = Na^2 - N^2a^2\left(\coth\zeta - \frac{1}{\zeta}\right)^2 \tag{7}$$

Susceptibility $\partial^2 F(f,T)/\partial f^2$ in force and temperature ensemble reads as follows,

$$\kappa = \frac{Na^2}{k_{\mathrm{B}}T}\left(\mathrm{csch}^2\zeta - \frac{1}{\zeta^2}\right) \tag{8}$$

In the next sections, one needs response of the chain in length and temperature ensemble which can be obtained by calculating the Helmholtz free energy via transformation $A(L,T) = F(f,T) + f\langle L\rangle$. The Helmholtz free energy of a polymer chain is given as follows,

$$A(L,T) = Nk_{\mathrm{B}}T\left(\zeta\coth\zeta - \log\left(4\pi a^2\frac{\sinh\zeta}{\zeta}\right) - 1\right) \tag{9}$$

Polymer chain in strong external force

Another interesting limiting case, is a very strong external force applied to the polymer chain. In this limit, the chain stretches extremely in the external force direction and the chain reaches the rod limit at sufficiently large external forces. The behavior of physical quantities under this extreme condition can be obtained by making limit of them when the external force approaches infinity as follows,

$$\begin{aligned}
\lim_{f\to\infty} F(f,T) &\to -\infty \\
\lim_{f\to\infty} \langle L\rangle &\to Na \\
\lim_{f\to\infty} \langle L^2\rangle &\to Na^2 \\
\lim_{f\to\infty} \Delta L^2 &\to Na^2 - N^2a^2 \\
\lim_{f\to\infty} \kappa &\to 0 \\
\lim_{f\to\infty} A(L,T) &\to \infty
\end{aligned} \tag{10}$$

The expectation value of the chain length goes to Na as it is expected from the rod limit. The squared chain length fluctuations goes to $Na^2 - N^2a^2$ as the rod limit is achieved, however, this is a negative value hence leads to an imaginary quantity for the fluctuations. Therefore, I would say at the rod limit the chain length fluctuations is not well defined. The susceptibility goes to zero i.e. the elasticity goes to infinity which means that the chain becomes a very stiff spring resembling the rod limit. Both of the free energies go to infinity at the rod limit.

Polymer chain in weak external force

In most biological situations, magnitude of the external force is much smaller than the thermal energy. In this limiting case, I can consider the dimensionless quantity $\zeta \ll 1$ and

make Taylor expansion over the physical quantities. The Taylor expansions give us the following terms,

$$F(f,T) = -Nk_{\mathrm{B}}T\log\left(4\pi a^2\right) - Nk_{\mathrm{B}}T\left(\frac{1}{6}\zeta^2 + O\left(\zeta^4\right)\right) \tag{11}$$

The first term in the canonical free energy is free energy of N freely rotating vectors in absence of the external force. The second term is the leading order term of the canonical free energy which contains the external force. This term has the most of information about a polymer chain.

$$\langle L\rangle = Na\left(\frac{1}{3}\zeta + O\left(\zeta^3\right)\right) \tag{12}$$

In Eqs. 12 and 13 average length and *compressiblity* of the chain is seen in weak external force. The leading order term in average length depends on external force so in absence of external force the average length vanishes as it is expected. Naturally, when a polymer chain is subject to an external force, it tends to align to the force direction. This causes non-zero average length which occurs in absence of external force.

$$\kappa = \frac{a^2N}{3k_{\mathrm{B}}T}\left(1 - \frac{1}{5}\zeta^2 + O\left(\zeta^4\right)\right) \tag{13}$$

The leading order term of compressibility is independent of external force. It gives an intrinsic property of polymer chain $\kappa^{-1} = \frac{3k_{\mathrm{B}}T}{a^2N}$ which indicates the elasticity originated from entropy. Looking at Eqs. 12 and 13, we see that the leading order term in the canonical free energy can be rewritten as $\frac{1}{2}\kappa^{-1}\langle L\rangle^2$. This is a free energy which introduces us *entropic* elasticity in a polymer chain. This term tries to shrink the chain. The inverse compressiblity or susceptibility plays role of spring constant in a chain. However, it is different from crystals. The elastic constant in crystalline solids decreases by increasing temperature but in a polymer chains and rubber-like materials the elastic constant increases upon increasing temperature. So, by heating up the polymers they contract due to $\langle L\rangle = f/\kappa^{-1}$ in contrast to crystalline materials.

$$\Delta L^2 = a^2N - N^2a^2\left(\frac{1}{9}\zeta^2 + O\left(\zeta^4\right)\right) \tag{14}$$

Fluctuation of chain length in weak external force is extremely interesting quantity. To find the leading order term in the perturbation expansion, we need to compare their order of magnitude. Since the second term is $\sim N^2$ it appears to dominate over the first term, however, it is multiplied by ζ^2. So find the leading order term, we need to make numerical comparison. Typical polymer chains consist $N = 10^5$ monomers and usually force is in order of pN, and typically, monomer size is 0.1 nm. Considering order of magnitude of the Boltzmann constant as 10^{-23} and room temperature $T = 300$K, the perturbation coefficient becomes $\zeta \sim 10^{-2}$. Consequently, the first and the second terms have almost the same order of magnitude and both of them are considered as leading order terms. As it is already expected, when temperature increases fluctuations of the chain length increases as well and in the extreme limit of $T \to \infty$ we have $\Delta L^2 \to a^2 N$. It means than fluctuations of the chain length equals to the expectation value of the squared chain length. Remarkably, in presence of the external force, fluctuations are small, as compared to the expectation value of the squared chain length, nevertheless, in absence of the external force, fluctuations equal to $\langle L^2 \rangle$. It means that under influence of the external force, the chain is stretched in the external force direction and shows minor fluctuations in length.

The Helmholtz free energy at small external force is given as follows,

$$A(L,T) = -Nk_{\mathrm{B}}T \log\left(4\pi a^2\right) + Nk_{\mathrm{B}}T\left(\frac{1}{6}\zeta^2 + O\left(\zeta^4\right)\right) \tag{15}$$

It shows that elasticity of a polymer chain is $\kappa^{-1}\langle L \rangle^2/2$ at small external forces. This is an significant result which will be used in the next section as the free energy of a polymer chain.

Polymer brushes

Polymer brushes are composed of linear polymer chains which are densely grafted onto a surface by one end[2]. The *steric* repulsion between monomers of nearby chains stretches the chains in perpendicular direction. Here, I review theory of polymer brushes based on the density functional theory[6,7]. Consider linear polymer chains that are grafted to a substrate at $z = 0$ (See Fig. (1)). Number of grafted chains per surface area is defined as the

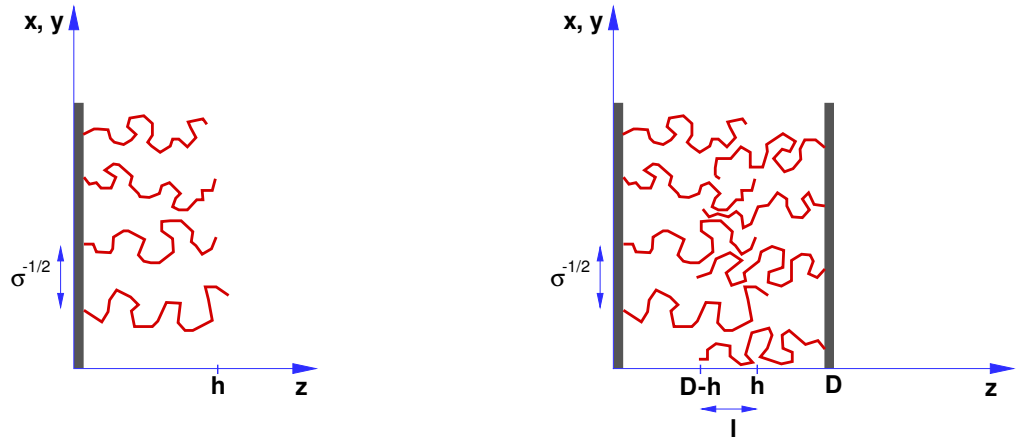

Figure 1: Schematic view of a polymer brush (left) and a polymer brush bilayer (right).

grafting density σ. Since, one deals with an in-homogeneous system, the grand potential is a functional of the density. The grand potential functional is given as follows,

$$\frac{\Phi[n(z)]}{k_{\mathrm{B}}T} = \int_0^h \left(\frac{3z^2}{a^2N^2}\, n(z) + b\, n(z)^2 - \mu\, n(z) \right) dz \tag{16}$$

The first term in Eq. 16 refers to leading order term of the Helmholtz free energy which describes the entropic elasticity of chains. Since energy is distributed throughout the chain according to the probability distribution function, one can multiply the Helmholtz free energy by $P(z) = n(z)/N$ with $n(z)$ the density profile of monomers. The second term refers to Virial expansion of the grand potential and it takes the excluded volume interactions among monomers into account. The third term applies a constraint over entire system to keep total number of monomers fixed with μ denoting the chemical potential.

The equilibrium density profile, brush height and chemical potential are obtained through simultaneous solution of the following coupled equations. The first equation sets a functional derivative of grand potential with respect to the monomer density profile. It leads to an Euler-Lagrange equation. Solution of the corresponding Euler-Lagrange equation gives us the equilibrium density profile. The second equation refers to derivative of grand potential with respect to brush height bearing the obtained equilibrium density profile. The third equation indicates that total number of monomers in brush is obtained through integration over density profile throughout brush region.

$$
\begin{aligned}
\frac{\delta\Phi[n(z)]}{(z)} &= 0 \\
\frac{\partial\Phi[n(z)]}{\partial h} &= 0 \\
\int_0^h n(z) &= N\sigma
\end{aligned}
\tag{17}
$$

Solving the set of coupled equations at Eqs. 17, gives us the following results,

$$
\begin{aligned}
n(z) &= \frac{3\sigma^{2/3}}{2a^{2/3}b^{1/3}} - \frac{3z^2}{2a^2N^2b} \\
h &= \frac{a^{2/3}b^{1/3}N\sigma^{1/3}}{2} \\
\mu &= 3k_{\mathrm{B}}T\left(\frac{b\sigma}{a}\right)^{2/3}
\end{aligned}
\tag{18}
$$

Eq. 18 reveals a parabolic density profile for brush as well as universal power laws for brush height and chemical potential in terms of molecular parameters. Inserting Eq. (22) into Eq. (17) gives us grand potential in terms of molecular parameters as follows,

$$
\Phi = -\frac{6}{5}Nk_{\mathrm{B}}T\left(\frac{b^{2/3}\,\sigma^{5/3}}{a^{2/3}}\right) \tag{19}
$$

which indicates that grand potential scales with molecular parameters as well.

RESULTS

Polymer brush bilayers

The most designated application for polymer brush bilayers is devoted to lubrication inside mammalian Synovial joints. In such a case, two opposing brush covered substrates are at a distance where brushes intermediately compressed over each other. Here, I consider two opposing brush covered surfaces at $z = 0$ and $z = D$ (See Fig. (1)). The following grand potential seems to be appropriate for this problem where the first integral represents the left side brush, the second integral represents the right side brush and the third integral represents the steric repulsion among monomers of two brushes throughout interpenetration

zone. The two brushes are exactly the same as each other in molecular parameters, so, to take the second brush into account, it suffices to transform $z \longrightarrow (z - D)$ in entropic elasticity term plus integrating from height of right brush $(D - h)$ to D. To take steric repulsion among two brush layers into account, we can integrate over a multiplication of both density profiles within the interpenetration zone i.e. from $(D - h)$ to h.

$$\begin{aligned}
\frac{\Phi[n(z), m(z)]}{k_{\mathrm{B}}T} &= \int_0^h \left(\frac{3z^2}{a^2N^2}\, n(z) + b\, n(z)^2 - \mu\, n(z) \right) dz \\
&+ \int_{D-h}^{D} \left(\frac{3(z-D)^2}{a^2N^2}\, m(z) + b\, m(z)^2 - \mu\, m(z) \right) dz \\
&+ b \int_{D-h}^{h} n(z)\, m(z)\, dz
\end{aligned} \tag{20}$$

Having introduced the grand potential functional, solving the following equations lead to equilibrium density profiles, brush height and chemical potential corresponding to each brush.

$$\begin{aligned}
\frac{\delta\Phi[n(z), m(z)]}{\delta n(z)} &= 0 \\
\frac{\delta\Phi[n(z), m(z)]}{\delta m(z)} &= 0 \\
\frac{\partial\Phi[n(z), m(z)]}{\partial h} &= 0 \\
\int_0^h n(z) &= N\sigma
\end{aligned} \tag{21}$$

Note here that, it suffices to take derivative of grand potential functional only with respect to h as well as to calculate total monomers of only left brush in calculations. This becomes possible due to similarity of two brushes. Eqs. 21 lead to the following results for monomer density profiles, brush heights and chemical potential. Note that, height of right brush is calculated as $(D - h)$.

$$
\begin{aligned}
n(z) &= \frac{\eta^2 + \frac{2D^3}{\eta} + 2D\left(\eta - 4z\right) + \frac{D^4}{\eta^2} - D^2 - 4z^2}{4a^2bN^2} \\
m(z) &= \frac{\eta^2 + \frac{2D^3}{\eta} + 2D\left(\eta + 8z\right) + \frac{D^4}{\eta^2} - 13D^2 - 4z^2}{4a^2bN^2} \\
h &= \frac{1}{2}\left(\eta + D\left(\frac{D}{\eta} - 1\right)\right) \\
\mu &= k_{\mathrm{B}}T\frac{3\left(2D\eta + \eta^2 + \frac{2D^3}{\eta} + \frac{D^4}{\eta^2} - 5D^2\right)}{4a^2N^2}
\end{aligned} \tag{22}
$$

where η is a length scale which is defined as follows,

$$
\eta = \left(\sqrt{6a^2bN^3\sigma\left(6a^2bN^3\sigma - 2D^3\right)} + 6a^2bN^3\sigma - D^3\right)^{1/3}
$$

Having brush heights, we can calculate the interpenetration length between two brushes through calculating $2h - D$. This calculation leads to the following result,

$$
l = \frac{\left(D - \eta\right)^2}{\eta} \tag{23}
$$

In Fig. 2, I present density profiles of brushes, their overlap density profile and density profile of an isolated brush Eq. (16) to show response of density profiles under compression. I choose molecular parameters as $a = 1$, $b = 2.09$, $\sigma = 0.1$, $N = 30$ and $D = 15$.

Density profiles of brushes at intermediate compression possesses three major properties; larger density of monomers in vicinity of surfaces, smaller thickness and non-parabolic (almost linear) behavior in z direction. These are considered as response of brushes to an intermediate compression through balancing *compressive* forces by interpenetration.

In Fig. 3, interpenetration length in terms of wall distance is presented. This plot, in contrast to what has been claimed in works already published, does not fit to any universal power law. However, interpenetration length decreases with increasing wall distance which is already expected. In Ref.[4], it is mentioned that the interpenetration length in polymer brush bilayers at melt concentration scales as $\sim D^{-1/3}$ and at semidilute concentration as $\sim D^{-0.17}$. However, the wall distance appears to not to fulfill similarity rules.

In Fig. 4, interpenetration length in terms of degree of polymerization is presented. I plot Eq. 23 and a power law fit as $\sim N^{0.976}$. This power law almost fits to Eq. 23. In Ref.[4],

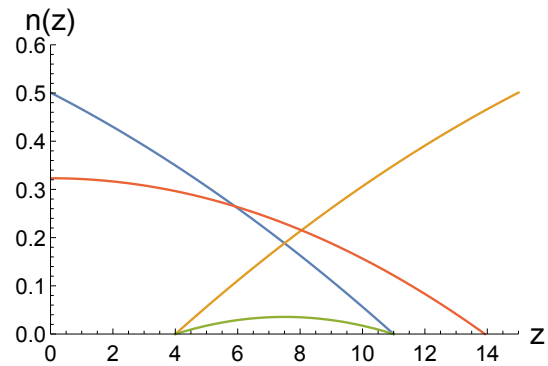

Figure 2: Density profiles of left brush (blue), right brush (orange), the overlap density profile of left and right brushes (green) and density profile of left brush in absence of right brush (red).

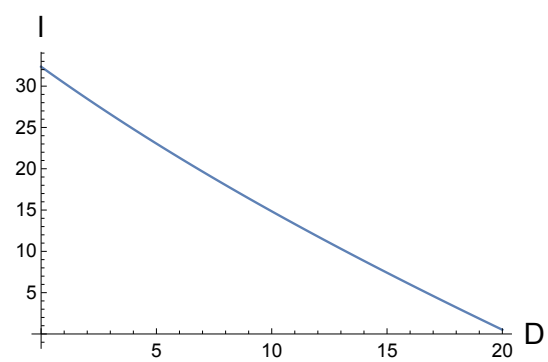

Figure 3: Interpenetration length in terms of wall distance.

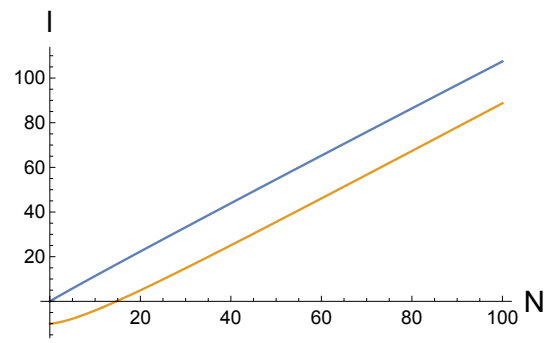

Figure 4: Interpenetration length in terms of degree of polymerization. Eq. 23 (orange) and universal scaling law $^{0.976}$ (blue).

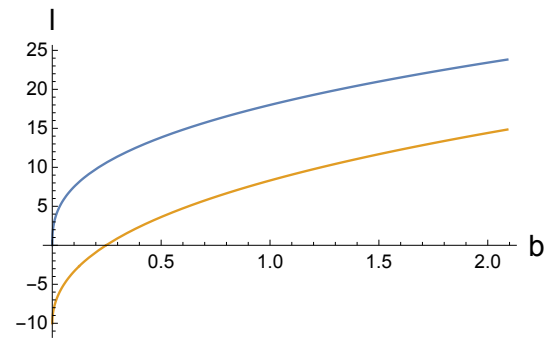

Figure 5: Interpenetration length in terms of the second Virial coefficient. Eq. 23 (orange) and universal power law $\sim b^{0.38}$ (blue).

universal power law $\sim N^{2/3}$ and $\sim N^{0.51}$ respectively for melt and semidilute regimes have been proposed. Naturally, as degree of polymerization increases, longer polymer chains tend to increase interpenetration length. Furthermore, the chains inside the interpenetration zone are not folded back. To this reason, the interpenetration length scales as $\sim N$.

In Fig. 5, I present interpenetration length in terms of the second Virial coefficient. Eq. 23 which fits to the power law $\sim b^{0.38}$. It is natural that bilayer respond to binary correlations among monomers. For instance, quality of solvent is determined by the second Virial coefficient as poor, theta or good solvent. In poor solvent conditions, monomers attract each other. As the second Virial coefficient vanishes in a certain temperature, a theta solvent appears in which the monomers do not go through binary correlations however there exists ternary and higher correlations among them[5]. As the second Virial coefficient increases the good solvent conditions appear[5].

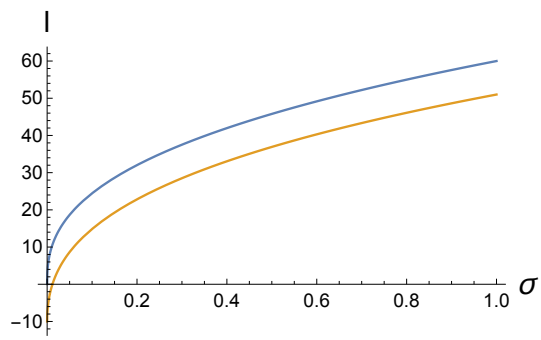

Figure 6: Interpenetration length in terms of the grafting density. Eq. 23 (orange) and universal power law $\sim \sigma^{0.39}$ (blue).

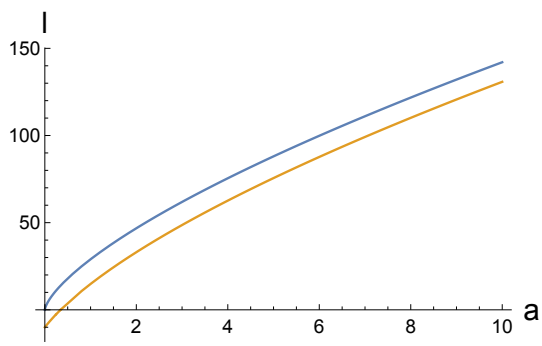

Figure 7: Interpenetration length in terms of the segment length. Eq. 23 (orange) and universal power law $\sim a^{0.69}$ (blue).

In Fig. 6, I show the interpenetration length in terms of the grafting density. This plot fits to power law $\sim \sigma^{0.39}$. In Ref.[4], the interpenetration length is independent of the grafting density for melts and it scales as $\sim \sigma^{-0.51}$ for semidilutes. However, one would criticize the results of Ref.[4] since the interpenetration length naturally must increase as number of chain per surface area increases.

In Fig. 7, I present the interpenetration length in terms of the segment length. This plot fits to power law $\sim a^{0.69}$. While Ref.[4] proposes a power law $\sim a^{4/3}$ for melts and $\sim a^{0.15}$ for semidilutes. The prediction of Ref.[4] about the interpenetration length at melt is quit close to my calculations.

The total grand potential can be calculated by inserting Eq. (22) into the grand potential and after integration we obtain,

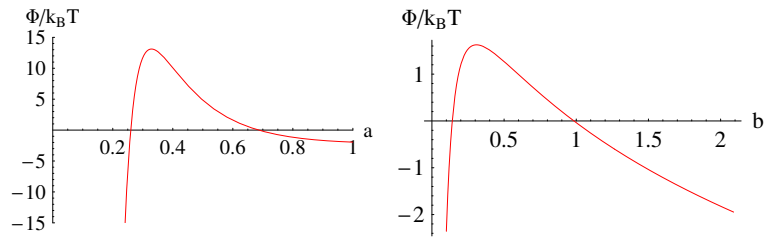

Figure 8: Total grand potential in terms of the segment length (left) and the second Virial coefficient (right).

$$\begin{aligned}\Phi = & - \frac{k_{\mathrm{B}}T}{240a^4bD^3N^4}(435D^8 + 720a^2bN^3\sigma - 187D^7\eta - 96a^2bDN^3\sigma\eta_1\eta \\ & + 187D^6\eta^2 - 300a^2bN^3\sigma\eta_1\eta^2 + D^4\eta_2\eta + 2D^3\eta_3\eta^2)\end{aligned} \tag{24}$$

where I introduce volumes as,

$$\begin{aligned}\eta_1 &= \left(\sqrt{6a^2bN^3\sigma\left(6a^2bN^3\sigma - 2D^3\right)} + 2a^2bN^3\sigma\right) \\ \eta_2 &= \left(151\sqrt{6a^2bN^3\sigma\left(6a^2bN^3\sigma - 2D^3\right)} - 702a^2bN^3\sigma\right) \\ \eta_3 &= \left(169\sqrt{6a^2bN^3\sigma\left(6a^2bN^3\sigma - 2D^3\right)} - 1116a^2bN^3\sigma\right)\end{aligned}$$

In Fig. (8), I present plots of Eq. (24) in terms of the segment length and the second Virial coefficient. Both quantities influence the grand potential in a way extremely similar to each other. At small segment lengths and the second Virial coefficients, the grand potential approaches $-\infty$. At the middle values, the grand potential energy possesses an unstable maximum positive value and at large values the grand potential energy again decreases to negative values and approaches a certain negative value. Existence of an unstable maximum point in the grand potential energy indicates that there is a certain segment length and the second Virial coefficient in which the total energy of the system maximizes. However, the system is very unstable in this point and with the smallest fluctuation drops down. Moreover, there are two zero energy points in the plots.

In Fig. (9), I present plots of Eq. (24) in terms of wall distance and the degree of polymerization. The grand potential in all wall distances is negative with a smooth minimum

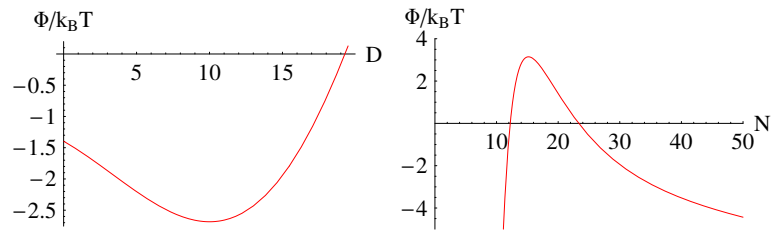

Figure 9: Total grand potential in terms of wall distance (left) and the degree of polymerization (right).

point in the middle. Existence this stable minimum point indicates that the substrates tend to stay in this distance. Practically, it means that there is a certain wall distance below which the substrates repel each other, however, above which they attract each other. Nevertheless, response of the grand potential under variation of the degree of polymerization is very similar to the segment length and the second Virial coefficient regarding existence of an unstable maximum point. Similarly, in a certain degree of polymerization, the system reaches its maximum possible energy but small fluctuations make system away from this maximum energy. With long chains, the energy of the system changes its sign and approaches an asymptotic value. In general, it appears that the molecular parameters corresponding to the chains i.e. the segment length, the second Virial coefficient and the degree of polymerization influence the total energy in the same way.

In Fig. (10), I show the grand potential in terms of the grafting density. The plot clearly indicates a universal power law in terms of grafting density. My fitting shows that the grand potential energy scales as $\sim \sigma^{1.5}$. It is showing that negativity of the grand potential energy increases by the grafting density. Practically, it means that the substrates are attracted by each other as the grafting density increases.

The energy due to binary correlations among monomers within the interpenetration region is obtained through inserting Eq. (22) into the third integral in Eq. (20) which gives us,

$$\begin{aligned}\Phi^l = & - \frac{k_{\mathrm{B}}T}{30a^4bD^3N^4}(42D^8 + 360a^2bD^5N^3\sigma - 11D^7\eta + 12a^2bDN^3\sigma\eta_1\eta \\ & + 11D^6\eta^2 + 60a^2bN^3\sigma\eta_1\eta^2 + 2D^3\eta_4\eta^2 + D^4\eta_5\eta) \end{aligned} \tag{25}$$

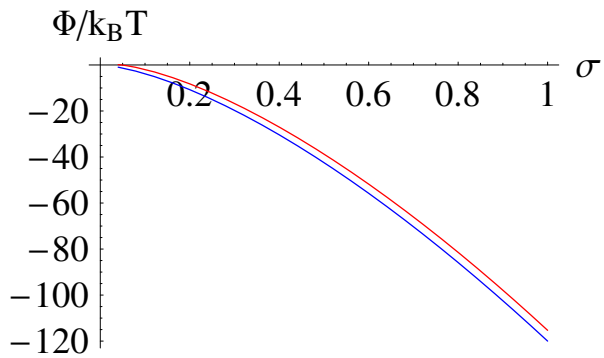

Figure 10: Total grand potential in terms of grafting density Eq. (24) (red), power law $\sim \sigma^{1.5}$ fit (blue).

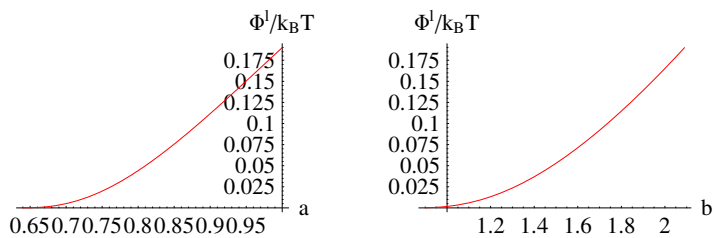

Figure 11: Energy within the interpenetration length in terms of the segment length (left) and the second Virial coefficient (right).

where I introduce volumes as,

$$\begin{aligned}\eta_4 &= \left(17\sqrt{6a^2bN^3\sigma\left(6a^2bN^3\sigma-2D^3\right)}-78a^2bN^3\sigma\right)\\ \eta_5 &= \left(23\sqrt{6a^2bN^3\sigma\left(6a^2bN^3\sigma-2D^3\right)}-186a^2bN^3\sigma\right)\end{aligned}$$

In Fig. (11), I present plots of Eq. (25) in terms of the segment length and the second Virial coefficient. The plots indicate that both parameters increase the energy within the interpenetration length.

In Fig. (12), I present plots of Eq. (25) in terms of the wall distance and the index of polymerization. In the case of variation of the index of polymerization, we observe a quit similar behavior with the segment length and the second Virial coefficient i.e. a non power law increment in energy. Nevertheless, the variation of wall distance influences the free energy within the interpenetration length as an increment at small distances, then an smooth

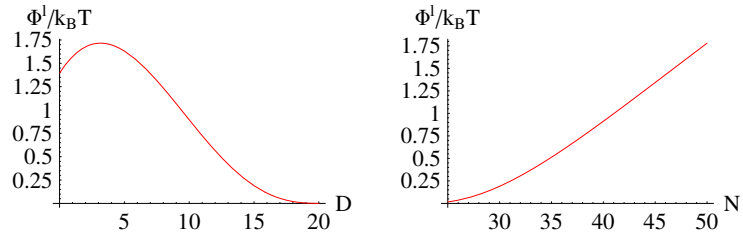

Figure 12: Energy within the interpenetration length in terms of the wall distance (left) and the degree of polymerization (right).

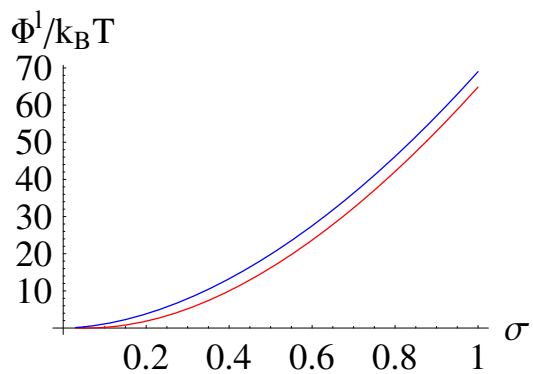

Figure 13: Energy within the interpenetration length in terms of the grafting density Eq. (25) (red), power law $\sim \sigma^{1.8}$ fit (blue).

maximum energy and subsequently, a reduction up to zero at large wall distances. Occurrence of a maximum point in a certain wall distance suggests that there is a threshold for the binary interactions among monomers within the interpenetration region. The threshold value occurs in large compression corresponding to small wall distances. The interesting outcome here is that the plot suggests that compressing more leads to less binary correlations among monomers withing the interpenetration region.

In Fig. (12), I present plots of Eq. (25) in terms of grafting density. Certainly, the plot indicates a power law. My fitting shows that the energy within the interpenetration length scales as $\sim \sigma^{1.8}$.

Taking derivative of Eq. (24) with respect to the wall distance produces the normal stress or pressure exerted on the bottom substrate at $z = 0$. Since, the system is at thermal equilibrium, the pressure is the same as throughout the medium. The derivative of the grand potential energy gives us the following pressure in terms of molecular parameters and wall

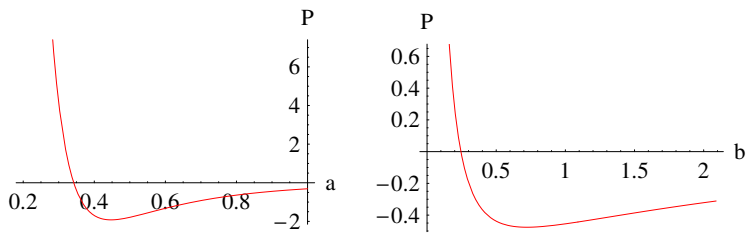

Figure 14: The normal stress or pressure exerted on the bottom substrate in terms of the segment length (left) and the second Virial coefficient (right).

distance,

$$
\begin{aligned}
P &= \frac{k_{\mathrm{B}}T}{48a^4bN^4\chi\eta^2}(720\sqrt{3}a^6b^3N^9\sigma^3 + D^4\chi(187D^2 - 187D\eta + 435\eta^2) \\
&+ 2a^2bDN^3\sigma(548\sqrt{3}D^5 - 852D^2\chi + 174\sqrt{3}D^4\eta - 231D\chi\eta + 144\chi\eta^2) \\
&+ 36a^4b^2N^6\sigma^2(10\chi - \sqrt{3}D^2(98D + 29\eta))) \qquad (26)
\end{aligned}
$$

where I introduce a volume χ as follows,

$$\chi = \sqrt{2a^2bN^3\sigma(6a^2bN^3\sigma - 2D^3)}$$

In Fig. (14), I present plots of Eq. (26) in terms of the segment length and the second Virial coefficient. In principle, both quantities influence the pressure similarly. At small values, there is a infinitely large pressure in z direction which decreases by the segment length and the second Virial coefficient. However, above those values, the pressure changes sign and orients in the negative z direction. After reaching an smooth maximum value in the negative z direction, the pressure again decreases and approaches a certain value.

In Fig. (14), I present plots of Eq. (26) in terms of the wall distance and the degree of polymerization. It shows that the pressure is upward at high compression, nevertheless, it is downward at low compression. However, at high compression there is a very smooth maximum pressure. It is also showing that the pressure changes its orientation in the moderate compression. The index of polymerization influences pressure in a way that with short chains, pressure is downward and infinitely large while with long chains, pressure becomes upward and reaches a certain asymptotic value.

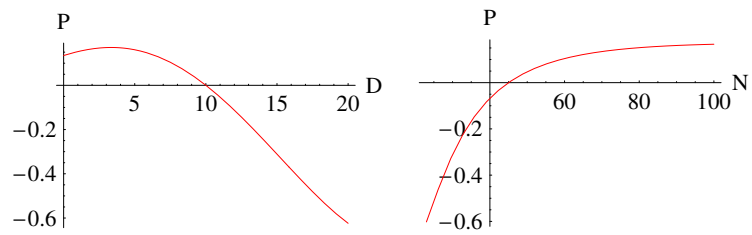

Figure 15: The normal stress or pressure exerted on the bottom substrate in terms of the wall distance (left) and the degree of polymerization (right).

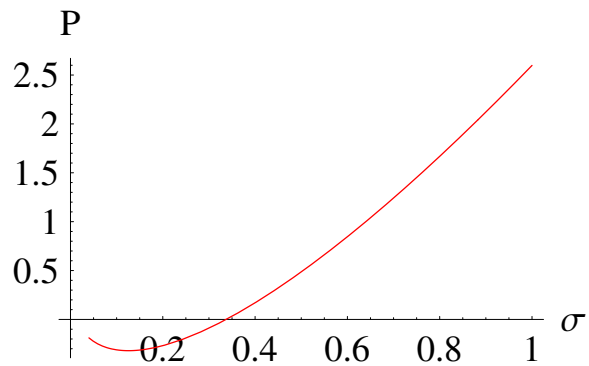

Figure 16: The normal stress or pressure exerted on the bottom substrate in terms of the grafting density.

In Fig. (16), I present plots of Eq. (26) in terms of the grafting density. At low grafting densities, pressure is downward and small, however, it changes sign in moderate grafting densities and becomes upward for large grafting densities.

CONCLUSIONS

In this study, I develop a theoretical model to approach the polymer brush bilayers. I show how polymer brushes interpenetrate with each other through giving approximate density profiles of two brushes. I also show how the interpenetration length depends upon molecular parameters and wall distance. The interpenetration length decreases by wall distance through a non-power law behavior. In contrast to previous publications, this suggests that the interpenetration length does not obey similarity rules in terms of wall distance. Although, it depends upon molecular parameters through universal power laws. All molecular

parameters follow similarity rules among them degree of polymerization influence the interpenetration length strongly, however, the grafting density and the second Virial coefficient have weak influences. Note here that, my calculations reveal that the interpenetration length scales linearly with degree of polymerization. This finding suggests that polymer chains in the interpenetration region do not fold back i.e. they are still in the strong stretching limit (SSL). Calculations indicate that all molecular parameters increase the interpenetration length though with different universal power laws. This is an interesting outcome, for instance, in the case of the second Virial coefficient which describes strength of the binary correlations among monomers. I have considered the strength of the binary correlations among all monomers as same as each other. One might say that increase in the interpenetration length due to the binary correlations occurs because of repulsion among monomers inside the brushes and not because of repulsion among monomers of different brushes within the interpenetration length. Nevertheless, if one takes different binary correlations among monomers of top and bottom brushes, presumably, it will be shown that the binary correlations among different brushes within the interpenetration length reduce it.

The total energy, the energy within the interpenetration region and the normal stress throughout the system indicate existence of zero energy and zero pressure points upon wide range of possible values for parameters of the system. This can be an application oriented outcome of this research, since, one might become able to tune pressure orientation through playing with the segment length, strength of the binary correlations (different solvent qualities) and chain length. The most interesting outcome, in this context, would be ability to change the pressure orientation via tuning distance between substrates. It would be fascinating in lubrication technology if someone become able to tune the friction coefficient by choosing right distance between surfaces. For instance, my study suggests that strongly compressed brushes attract each other, nevertheless, weakly compressed brushes repel each other. So, one might only use weakly compressed brush covered surfaces for lubrication purposed. Another suggestion of this research would be to use short chains and lower grafting density to achieve repulsion of substrates. The reason for this claim is hidden in the complex interactions among monomers.

Significance of this study becomes more clear as it is a unique approach to problem of

interpenetration of two soft materials by taking their simultaneous deformations into account. Simultaneous deformation is a key element in approaching soft matter and biological systems. The blob picture which have been utilized in Ref.[4] seems to be extremely simple and it does not capture important details. For instance, interpenetration length is dependent upon binary correlations among monomers as well as it increases by grafting density, two facts that blob picture does not take into account. It is worth noting that since in biological macromolecules there are competitions among different interactions (such as elasticity, excluded volume etc), therefore approaches like blob picture are not able, intrinsically, to deliver sufficient information.

References

1. Rubinstein, M. and Colby, R.H., Polymer Physics, OUP Oxford (2003)

2. Advincula, R.C. and Brittain, W.J. and Caster, K.C. and Rühe, J., Polymer Brushes, Wiley-VCH, Weinheim (2004)

3. Schwabl, F. and Brewer, W.D., Statistical Mechanics, Advanced Texts in Physics, Springer Berlin Heidelberg, 313-316 (2006)

4. Kreer, T, Polymer-brush lubrication: a review of recent theoretical advances, Soft Matter, 12, 3479 (2016)

5. Gennes, Pierre Gilles, Scaling Concepts in Polymer Physics, Cornell University Press, 74-75 (1979)

6. Hirz, S. J., Modeling of Interactions Between Adsorbed Block Copolymers, University of Minnesota, Minneapolis, MN (1988)

7. Safran, S., Statistical Thermodynamics Of Surfaces, Interfaces, And Membranes, Boca Raton: CRC Press. (2003)